Long non-coding RNA DANCR aggravates breast cancer through the miR-34c/E2F1 feedback loop

SHUAI YAN[1-4], LIZHI TENG[1,2,4], JUNTONG DU[1,2,4], LIANG JI[1-4], PENG XU[1,2,4], WENXI ZHAO[1,2,4] and WEIYANG TAO[1-4]

[1]Department of Breast Surgery, The First Affiliated Hospital of Harbin Medical University; [2]Key Laboratory of Acoustic, Optical and Electromagnetic Diagnosis and Treatment of Cardiovascular Diseases, Harbin Medical University; [3]Key Laboratory of Hepatosplenic Surgery, Ministry of Education, Harbin Medical University; [4]The Cell Transplantation Key Laboratory of National Health Commission, Harbin Medical University, Harbin, Heilongjiang 150001, P.R. China

Received October 21, 2023; Accepted March 11, 2024

DOI: 10.3892/mmr.2024.13217

Abstract. Emerging scientific evidence has suggested that the long non-coding (lnc)RNA differentiation antagonizing non-protein coding RNA (*DANCR*) serves a significant role in human tumorigenesis and cancer progression; however, the precise mechanism of its function in breast cancer remains to be fully understood. Therefore, the objective of the present study was to manipulate *DANCR* expression in MCF7 and MDA-MB-231 cells using lentiviral vectors to knock down or overexpress *DANCR*. This manipulation, alongside the analysis of bioinformatics data, was performed to investigate the potential mechanism underlying the role of *DANCR* in cancer. The mRNA and/or protein expression levels of *DANCR*, *miR-34c-5p* and E2F transcription factor 1 (*E2F1*) were assessed using reverse transcription-quantitative PCR and western blotting, respectively. The interactions between these molecules were validated using chromatin immunoprecipitation and dual-luciferase reporter assays. Additionally, fluorescence *in situ* hybridization was used to confirm the subcellular localization of *DANCR*. Cell proliferation, migration and invasion were determined using 5-ethynyl-2'-deoxyuridine, wound healing and Transwell assays, respectively. The results of the present study demonstrated that *DANCR* had a regulatory role as a competing endogenous RNA and upregulated the expression of *E2F1* by sequestering *miR-34c-5p* in breast cancer cells. Furthermore, *E2F1* promoted *DANCR* transcription by binding to its promoter in breast cancer cells. Notably, the *DANCR*/*miR-34c-5p*/*E2F1* feedback loop enhanced cell proliferation, migration and invasion in breast cancer cells. Thus, these findings suggested that targeting *DANCR* may potentially provide a promising future therapeutic strategy for breast cancer treatment.

Correspondence to: Professor Weiyang Tao, Department of Breast Surgery, The First Affiliated Hospital of Harbin Medical University, 23 Youzheng Street, Nangang, Harbin, Heilongjiang 150001, P.R. China
E-mail: twysci@outlook.com

Key words: differentiation antagonizing non-protein coding RNA, microRNA-34c, E2F transcription factor 1, competing endogenous RNA, breast cancer

Introduction

There are >1.6 million new cases of breast cancer diagnosed each year, making it the most common malignancy among women worldwide (1). Breast cancer metastasis is a life-threatening occurrence that constitutes the primary cause of breast cancer-related deaths (2). Previous studies have aimed to identify the molecular processes that cause breast cancer metastasis and to search for new targets that can stop its progression (3,4). The specific underlying mechanisms driving cell migration and invasion remain largely unknown, despite the crucial role they serve in the metastatic development of breast cancer.

According to previous studies, long non-coding RNAs (lncRNAs) serve an important role in human cancer (5,6). Numerous types of human cancer cells exhibit dysregulated expression of these ncRNA molecules, which are ~200 nucleotides in length and are transcribed from the corresponding gene locus (7,8). LncRNAs exert biological functions through the epigenetic modulation of transcriptional and post-transcriptional regulation in physiological and pathological activities. Notably, lncRNAs are essential regulators in human cancer and have a substantial association with tumor prognosis (9,10).

The lncRNA differentiation antagonizing non-protein coding RNA (*DANCR*) was initially reported to be associated with osteoclastogenesis and osteoblast differentiation in osteoporosis (11). It has also been reported that *DANCR* is overexpressed in neoplastic tissues and functions as an oncogenic lncRNA by facilitating the development of tumors (12). Previous research has reported that lncRNAs are involved in the epigenetic modification of multiple diseases, including both transcriptional and post-transcriptional regulation (5,6). In the present study, the association between *DANCR* and E2F transcription factor 1 (*E2F1*) expression is assessed. However, to the best of our knowledge, there has been no research to date reporting the mechanism underlying the relationship

between *DANCR* and *E2F1* in cancer; therefore, the present study aimed to elucidate the oncogenic function of *DANCR* in cancer.

Materials and methods

The Cancer Genome Atlas (TCGA) data access and analysis. *DANCR* and other gene expression profiles and clinicopathological factors were downloaded from TCGA (Data Release v21.0; December 10, 2019) (https://tcga-data.nci.nih.gov/). To analyze the expression levels of *DANCR*, the data were dichotomized using the median expression as the cut-off point, defining 'high' as expression levels at or above the median and 'low' as expression levels below the median. The log-rank test was used to assess differences in survival between different groups of patients.

Human DNA methylation profiles were determined experimentally using the Illumina Infinium Human Methylation 450 platform (Illumina, Inc.). β-values were obtained from Johns Hopkins University and TCGA Genome Characterization Center of the University of Southern California (California, USA). DNA methylation and β-values of each array probe were measured across all samples using the BeadStudio (version 3.2; Illumina, Inc.) software. The β-values varied from 0-1, which represented the ratio of the methylated bead type to the combined locus intensity. Consequently, increased β-values indicated increased DNA methylation levels, while decreased β-values indicated decreased DNA methylation levels. These values were treated as continuous variables. Additionally, information about histone modifications of the *DANCR* locus was retrieved from the ENCODE database (ENCODE 3 Nov 2018) (https://www.encodeproject.org/).

Transcription factor (TF) prediction and guilt-by-association analysis. The JASPAR database (https://Jaspar.bind.Ku.dk/) was used to predict TFs and the chromatin immunoprecipitation (ChIP)-seq data obtained from ENCODE served as the basis for analysis.

According to previous investigations, the guilt-by-association methodology was adopted to discern genes that exhibited a positive correlation with *DANCR* (13-16). The pairwise Pearson correlation was applied to measure the correlation between *DANCR* expression and that of other genes. As a result, solely the genes that exhibited a favorable association with a correlation coefficient of $R \geq 0.3$ and attained statistical significance at a level of $P<0.05$ were chosen. Subsequently, DAVID Functional Annotation Bioinformatics Microarray Analysis (https://david.ncifcrf.gov/tools.jsp) was performed based on Kyoto Encyclopedia of Genes and Genomes (KEGG) pathways and Gene Ontology (GO) terms. $P<0.05$ and a gene count threshold of 4 were used to identify significant GO terms and KEGG pathways.

Human tissue specimens and ethics statement. The present study acquired five paired samples of breast cancer tissues and their respective adjacent noncancerous tissues (mean patient age, 58±13 years) as well as information on patient sex, age, patient number and molecular subtypes from The First Hospital of Harbin Medical University (Harbin, China). Patients with *DANCR* information were eligible for the present study, which met the ethical standards of The Declaration of Helsinki.

For RNA isolation, tissue samples were collected from patients with breast cancer and healthy controls (n=5/group) and immediately cryopreserved at -80˚C after resection. Before surgery, written informed consent was obtained from all patients. Patients with a history of adjuvant chemotherapy, immunotherapy, radiotherapy, tumor recurrence, bilateral tumor, metastatic disease or other previous tumors were excluded from the present study. The Ethics Committee of the First Affiliated Hospital of Harbin Medical University (Harbin, China) granted ethical approval after obtaining written informed consent from patients (ethical approval no. 202438).

Cell culture. MCF7 (cat. no. HTB22), MDA-MB-231 (cat. no. CRM-HTB-26), MCF10A (cat. no. CRL-10317) and 293T (cat. no. ACS-4500) cell lines were obtained from the American Type Culture Collection. MCF7, MCF10A and 293T cell lines were maintained in DMEM (Gibco; Thermo Fisher Scientific, Inc.) and MDA-MB-231 was maintained in L15 (Gibco; Thermo Fisher Scientific, Inc.) for culture purposes. Before the experiments, the cells were tested to rule out the presence of *Mycoplasma*. Cells were cultured at 37˚C in a humidified environment with 10% FBS (Gibco; Thermo Fisher Scientific, Inc.) and 5% CO_2.

Cell transfection. Small interfering (si)RNAs targeting *DANCR*, si*DANCR* negative control (NC; cat. no. siN0000001-1-5), siRNAs targeting *E2F1*, si*E2F1* NC, miRNA mimics, miRNA inhibitors, mimic NC (cat. no. miR1N0000001-1-5) and inhibitor NC (cat. no. miR2N0000001-1-5) were purchased from Guangzhou RiboBio Co, Ltd. The *DANCR* plasmid (pcDNA3.1-*DANCR*) was constructed by Shanghai GeneChem Co., Ltd. for DANCR overexpression. The experimental procedure involved seeding $1x10^5$ cells into a 6-well plate and transfecting cells when they reached a confluence of 70-80%. Transfection was performed using JetPRIME (Polyplus-transfection SA) and different masses of nucleic acids as follows: *DANCR* overexpression plasmid (2,000 ng); miRNA inhibitor (50 nmol); siRNA (100 nmol); and miRNA mimic (100 nmol) for 24 h at 37˚C and 5% CO_2. The transfected cells were employed for subsequent experimentations at 24 h after transfection. The transfection efficiency was determined using reverse transcriptase-quantitative (RT-q) PCR and western blotting analysis at 24 and 48 h after the transfection, respectively. The sequences used were as follows: si*DANCR*#1 sense, 5'-CCAACUAUCCCUUCAGUUA-3' and antisense, 5'-UAACUGAAGGGAUAGUUGG-3'; si*DANCR*#2 sense, 5'-GUGCUUCAUGUUCACCUUU-3' and antisense, 5'-AAAGGUGAACAUGAAGCAC-3'; si*E2F1* sense, 5'-GGGAGAAGUCACGCUAUGA-3' and antisense, 5'-UCAUAGCGUGACUUCUCCC-3'; hsa-*miR-34c-5p* mimic sense, 5'-AGGCAGUGUAGUUAGCUGAUUGC-3' and antisense, 5'-GCAAUCAGCUAACUACACUGCCU-3'; and hsa-*miR-34c-5p* inhibitor, 5'-GCAAUCAGCUAACUACACUGCCU-3'.

Lentiviral infection. DANCR-specific short-hairpin (sh)RNA-targeting coding sequences and non-targeting negative control sequences (Shanghai GeneChem Co., Ltd.) were

cloned into GV112 vectors (Shanghai GeneChem Co., Ltd.) to produce DANCR knockdown vectors. The shDANCR sequence used in the experiment was as follows: 5'-GTGCTT CATGTTCACCTTT-3'. The NC of shDANCR sequence used in the experiment was as follows: 5'-TTCTCCGAACGTGTC ACGT-3'. A 3rd generation system was used to package the lentivirus. To produce lentiviral particles, TransIT-LT1 (Mirus Bio, LLC) was used to co-transfect the expression vector with the packaging plasmid pHelper 1.0 (Shanghai GeneChem Co., Ltd.) and the envelope plasmid pHelper 2.0 (Shanghai GeneChem Co., Ltd.) into 293T cells at 37˚C and 5% CO_2 for 24 h. The supernatant was collected 48 h post-transfection and concentrated using ultracentrifugation at 75,500 x g and 4˚C for 90 min and resuspended in an appropriate volume of OptiMEM (Gibco; Thermo Fisher Scientific, Inc.). MCF7 and MDA-MB-231 cells were seeded in 6-well plates at a density of $1x10^5$ cells/well and cultured in DMEM with 10% FBS at 5% CO_2 at 37˚C and transfecting cells when they reached a confluence of 70-80%. The cells were transfected with 10 μg lentiviral plasmids, 7.5 μg packaging plasmid and 5 μg envelope plasmid at a multiplicity of infection of 10 using Lipofectamine® 2000 (Invitrogen; Thermo Fisher Scientific, Inc.) the following day when the cells were ~70% confluent. MCF7 and MDA-MB-231 cells were cultured at 37˚C for 6 h followed by replacement of the medium. The cells were incubated at 37˚C for 48 h and subsequently treated with puromycin (selection, 2 μg/ml; maintenance, 1 μg/ml; Calbiochem; Merck KGaA) at 37˚C and 5% CO_2 for 72 h to select transfected clones. Stable knockdown of DANCR was confirmed by RT-qPCR.

Proliferation assay. Cell proliferation was assessed using the 5-ethynyl-2'-deoxyuridine (EdU) assay (Beyotime Institute of Biotechnology), following the manufacturer's instructions. After a 4-h incubation with EdU, the cells were fixed in 4% formaldehyde for a duration of 30 min at room temperature. Then, a glycine solution (2 mg/ml) was applied for 5 min, followed by permeabilization using 0.5% Triton X-100 for 10 min at room temperature. A 1X reaction cocktail (from EdU kit) was then administered and the nuclei were stained with DAPI for 10 min at room temperature. The cells were then imaged under a fluorescence inverted microscope.

Wound healing assay. A wound healing assay was conducted to examine MCF7 and MDA-MB-231 cell migration. Initially, $1x10^5$ cells were seeded in a 6-well plate and incubated until they reached ~100% confluence at 5% CO_2 and 37˚C. The cells were then scratched using a pipette tip to create wounds and the concentration of FBS in the cell culture medium was reduced from 10% to 1%. An image of the scratched area was immediately taken (0 h). The plates were then placed at 37˚C and 5% CO_2. After overnight (16-h) incubation, another image was taken of the same scratched area using light microscopy (magnification, x10). The width of the scratch at 24 h was calculated as a percentage of the width at 0 h. The cell migration rate was analyzed by the edge-finding method using Image J 1.8.0 (National Institutes of Health).

Invasion assay. MCF7 ($1x10^5$) and MDA-MB-231 ($1x10^5$) cells were incubated in serum-free DMEM or RPMI-1640 (Gibco; Thermo Fisher Scientific, Inc.) medium using the BRAND® Insert with Matrigel (cat. no. BR782806; MilliporeSigma; Merck KGaA) precoated for 4 h and 37˚C. Serum-free medium was added to both upper chambers and medium containing 10% FBS was added to the lower cell chamber. After 24 h of incubation at 37˚C, RPMI-1640 or DMEM containing 10% FBS was added to the lower chamber and non-invading cells were removed with a cotton swab. Cells that successfully traversed the membrane were immobilized in 100% methanol for 30 min and subsequently dehydrated by air drying. Furthermore, these cells were stained with a 0.5% crystal violet solution at room temperature for 30 min and counted manually after imaging using a light microscope.

RNA preparation and RT-qPCR. TRIzol® reagent (Invitrogen; Thermo Fisher Scientific, Inc.) was used to extract total RNA from cells and tissue. Subsequently, PrimeScript RT Reagent Kit (Takara Bio, Inc.) was used to reverse transcribe 0.5 μg total RNA. FastStart Universal SYBR Green Master Mix (Roche Applied Science) and gene-specific primers were used, with *U6* or *GAPDH* used as internal controls. The ABI 7500 Fast Real-time PCR Detection System (Applied Biosystems; Thermo Fisher Scientific, Inc.) was used for RT-qPCR. To normalize the results, expression levels relative to *GAPDH* and *U6* were assessed using the $2^{-\Delta\Delta Cq}$ method (17). The miRNA stem-loop real-time PCR kit (Guangzhou RiboBio Co., Ltd.) was used to quantify *miR-34c-5p* and *U6*. The primer sequences were as follows: *DANCR* forward (F), 5'-CGGAGG TGGATTCTGTTAGGGACA-3' and reverse (R), 5'-AGAGGG CTTCGGTGTAGCAAGT-3'; *E2F1* F, 5'-GGACCTGGAAAC TGACCATCAG-3' and R, 5'-CAGTGAGGTCTCATAGCG TGAC-3'; U6 F, 5'-CTCGCTTCGGCAGCACAT-3' and R, 5'-TTTGCGTGTCATCCTTGCG-3'; and GAPDH F, 5'-GTC TCCTCTGACTTCAACAGCG-3' and R, 5'-ACCACCCTG TTGCTGTAGCCAA-3'. The thermocycling conditions were as follows: Initial denaturation at 95˚C for 10 min; 40 cycles at 95˚C for 15 sec and 60˚C for 30 sec.

Western blotting analysis. Protease and phosphatase inhibitors (Beyotime Institute of Biotechnology) were added to the RIPA (Beyotime Institute of Biotechnology) to lyse the MCF7 and MDA-MB-231 cells. The protein concentrations were measured using a BCA Protein Assay Kit (Beyotime Institute of Biotechnology). Subsequently, equivalent quantities of protein (30 μg) was loaded per lane onto a 10% SDS gel, resolved using SDS-PAGE and translocated onto nitrocellulose membranes, followed by blocking with 5% milk in TBST (0.1% Tween) at room temperature for 2 h. Primary antibodies targeting *E2F1* (1:1,000; cat. no. 3742; CST Biological Reagents Co., Ltd.) and *β-actin* (1:1,000; cat. no. TA09; OriGene Technologies, Inc.) were incubated with the membranes at 4˚C overnight. Primary antibodies were then washed away with TBST (0.1% Tween), incubated with IRDye 800CW-conjugated secondary antibodies (1:10,000; cat. no. 92632210/92632211; LI-COR Biosciences) for 1 h at room temperature and visualized using the Odyssey® Imaging System and Image Studio (LI-COR Biosciences).

ChIP assay. The ChIP detection kit (cat. no. bes5001, Guangzhou Bersinbio Co., Ltd.) was used with slight

modifications to the manufacturer's protocol (18). Cells were crosslinked using 1% formaldehyde and the reaction was terminated by adding glycine to a final concentration of 0.125 M. The *E2F1* antibodies (1:100) were used to immunoprecipitate DNA from sonicated cell lysates, with IgG (BD Biosciences) as the negative control. To detect the binding sites of *E2F1*, the immunoprecipitated DNA was amplified by RT-qPCR, as aforementioned. Subsequently, 3% agarose gel electrophoresis was used to analyze the amplified fragments. Chromatin at a concentration of 10% was used as a control input before immunoprecipitation. The primer sequences were as follows: *DANCR* site 1 F, 5'-CGGGGATTGGTAGGTAGCC-3' and R, 5'-CTGGAGAGGTCGGGTAGC-3'; *DANCR* site 2 F, 5'-GGT GTCCCCACGAGCTTTG-3' and R, 5'-AAATTGTTACGG TGCCCAGAC-3'; and *DANCR* site 3 F, 5'-CGCCCCGCT CAGGATCTTC-3' and R, 5'-GCACTCACCGCGCAACTC-3'.

Dual-luciferase reporter assay. To produce reporter vectors with binding sites for miRNA, the complete 3' untranslated regions (UTRs) of human *DANCR* and *E2F1* were cloned. The full-length 3'UTR fragments from *DANCR* and *E2F1* were amplified by PCR as aforementioned and inserted into the reporter luciferase expression vector pmiR-RB with *Not*1-*Xho*1 sites. 293T cells were cultured in DMEM containing 100 μg/ml penicillin/streptomycin and 10% FBS and *miR-34c-5p* mimic was used for the luciferase assay. 293T cells were transfected at 40-50% confluence using JetPRIME (Polyplus-transfection SA). For transfection, 20 mol/l hsa-*miR-34c-5p* mimic or NC, alongside 0.5 mg *DANCR* or *E2F1* plasmid (Guangzhou RiboBio Co., Ltd.), was utilized. The results of the luciferase activity were determined after 48 h using a luminometer (GloMax™ 20/20; Promega Corporation) and a dual-luciferase reporter assay kit (Promega Corporation). The direct oligomer synthesis technique was employed to produce a nucleotide-substitution mutation in the 3'UTRs of *DANCR* and *E2F1*. Normalization of the firefly luciferase results was performed by comparison with *Renilla* luciferase activity.

Prediction of lncRNA localization and fluorescence in situ hybridization (FISH). The lncRNA subcellular localization predictor database (lncLocator; http://www.csbio.sjtu.edu.cn/bioinf/lncLocator/) was used to analyze the subcellular localization of *DANCR*. FISH was performed using a RNA-FISH kit (Bes1002; Guangzhou BersinBio Biotechnology Co., Ltd.) as described in the manufacturer's instructions (19). The lncRNA probe for *DANCR* was obtained from Guangzhou Bersinbio Biotechnology Co., Ltd. MCF7 and MDA-MB-231 cells were harvested and fixed in 4% formaldehyde. After denaturation, probes were hybridized with cells for 20 h at 42˚C. A DAPI stain was then applied to the nuclei and cells were observed using a fluorescence microscope (LSM800; Carl Zeiss AG).

Statistical analysis. All statistical tests were conducted utilizing R (version 3.5.3; RStudio, Inc.). The data were presented as the mean ± standard deviation from three independent replicates. The expression of DANCR in cancer tissues compared with normal tissues were analyzed using a paired t-test. The unpaired Student's t-test was used to compare variances between two groups. For evaluating statistical differences among multiple groups, a one-way ANOVA was performed, followed by a Tukey's Honestly Significant Difference post hoc test. $P<0.05$ was considered to indicate a statistically significant difference.

Results

Upregulation of DANCR correlates with poor prognosis in breast cancer. TCGA data were downloaded and analyzed to evaluate the expression levels of *DANCR* in human cancer. These results demonstrated that the expression levels of *DANCR* were upregulated in pan-cancer samples when compared with normal samples (Fig. 1A; Table SI). Additionally, it was demonstrated that the expression levels of *DANCR* were notably elevated in various types of malignancy, including bladder urothelial carcinoma (BLCA), cholangiocarcinoma, colon adenocarcinoma, liver hepatocellular carcinoma (LIHC), lung adenocarcinoma, lung squamous cell carcinoma, prostate adenocarcinoma (PRAD), rectum adenocarcinoma, uterine corpus endometrial carcinoma (UCEC) and breast invasive carcinoma (BRCA), when compared with their noncancerous tissue counterparts (Fig. 1B; Table SI). To verify this observation, RT-qPCR analysis of breast cancer tissues was conducted and yielded results consistent with the aforementioned findings (Fig. 1C; Table SII).

The relationship between *DANCR* expression levels and patient survival status was further investigated using a log-rank test and Kaplan-Meier analysis based on pan-cancer samples. The results demonstrated that, compared with patients with low *DANCR* expression, patients with high expression had markedly lower disease-specific survival and overall survival (OS) (Fig. 1D). Furthermore, *DANCR* expression was significantly higher in advanced TNM stages than in stage I (Fig. 1E). Patients with high *DANCR* expression had significantly lower OS compared with patients with low DANCR expression, especially in patients with breast cancer (Fig. 1F). Furthermore, compared with other subtypes of breast cancer, the expression of *DANCR* was significantly upregulated in the triple negative subtype (Fig. 1G). In addition, various cancer types present in the TCGA data cohort were examined. The analysis demonstrated a notable correlation between elevated levels of *DANCR* in BRCA, kidney renal clear cell carcinoma, LIHC, sarcoma and skin cutaneous melanoma and a decline in OS rates (Figs. 1F and S1). However, the expression of *DANCR* in Head and Neck squamous cell carcinoma (HNSC), Kidney Chromophobe, Pheochromocytoma and Paraganglioma, Stomach adenocarcinoma, Thyroid carcinoma (THCA) and UCEC was not linked to OS (Fig. S1).

DANCR promoted tumor growth. To elucidate the role of *DANCR* in the phenotype of breast cancer cells, loss-of-function experiments were conducted on MCF7 and MDA-MB-231 breast cancer cells. After transfection with siRNA, the expression of *DANCR* in these cells was significantly decreased compared with control cells (Fig. 2A). In addition, after stable silencing of *DANCR*, the EdU assay showed a decrease in proliferation compared with control cells, whereas the opposite results were determined after overexpression of *DANCR* (Fig. 2B). These findings suggested that *DANCR* knockdown can inhibit breast cancer cell proliferation, implying a potential oncogenic role in tumorigenesis.

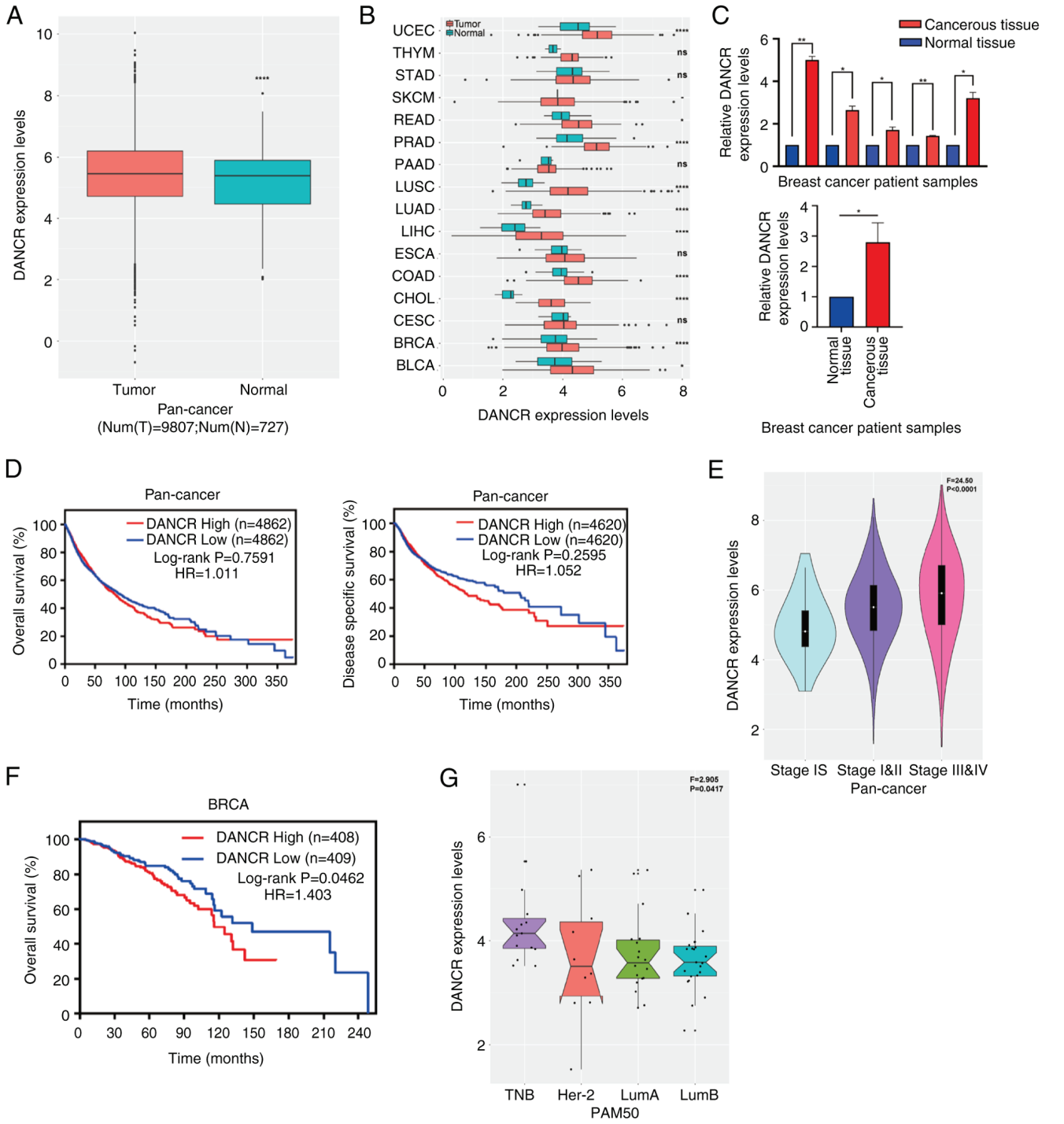

Figure 1. Expression of *DANCR* is upregulated and correlated with a poor prognosis. (A) Expression level of *DANCR* was significantly higher in pan-cancer tissues when compared with normal tissues. (B) The Cancer Genome Atlas results demonstrated that the expression level of *DANCR* was significantly higher in UCEC, SKCM, READ, PRAD, LUSC, LUAD, LIHC, ESCA, COAD, CHOL, BRCA and BLCA and markedly higher in THYM, STAD, PAAD and CESC compared with normal tissues. (C) Expression level of *DANCR* was higher in breast cancer tissues compared with normal tissue (n=5/group). Higher *DANCR* expression level had a significant positive association with (D) poor overall survival, a marked positive association with poor disease-specific survival and a significant positive association with (E) advanced stage in pan-cancer. (F) Higher expression level of *DANCR* was significantly related to poorer overall survival in BRCA. (G) *DANCR* expression was upregulated in triple-negative and HER-2 enriched subtypes. *P<0.05; **P<0.01; *****P<0.0001. DANCR, differentiation antagonizing non-protein coding RNA; UCEC, uterine corpus endometrial carcinoma; THYM, thymoma; STAD, stomach adenocarcinoma; SKCM, skin cutaneous melanoma; READ, rectum adenocarcinoma; PRAD, prostate adenocarcinoma; PAAD, pancreatic adenocarcinoma; LUSC, lung squamous cell carcinoma; LUAD, lung adenocarcinoma; LIHC, liver hepatocellular carcinoma; ESCA, esophageal carcinoma; COAD, colon adenocarcinoma; CHOL, cholangiocarcinoma; CESC, cervical squamous cell carcinoma and endocervical adenocarcinoma; BRCA, breast invasive carcinoma; BLCA, bladder urothelial carcinoma; TNB, triple-negative breast cancer; Her-2, human epidermal growth factor receptor 2; LumA, luminal A; LumB, luminal B; HR, hazard ratio; PAM 50, PAM 50 molecular subtype; num(T), number of tumor tissues; num(N), number of normal tissues.

Subsequently, an evaluation was conducted to determine the impact of *DANCR* on breast cancer cell migration and invasion through the implementation of wound healing and Transwell assays. The findings demonstrated that the

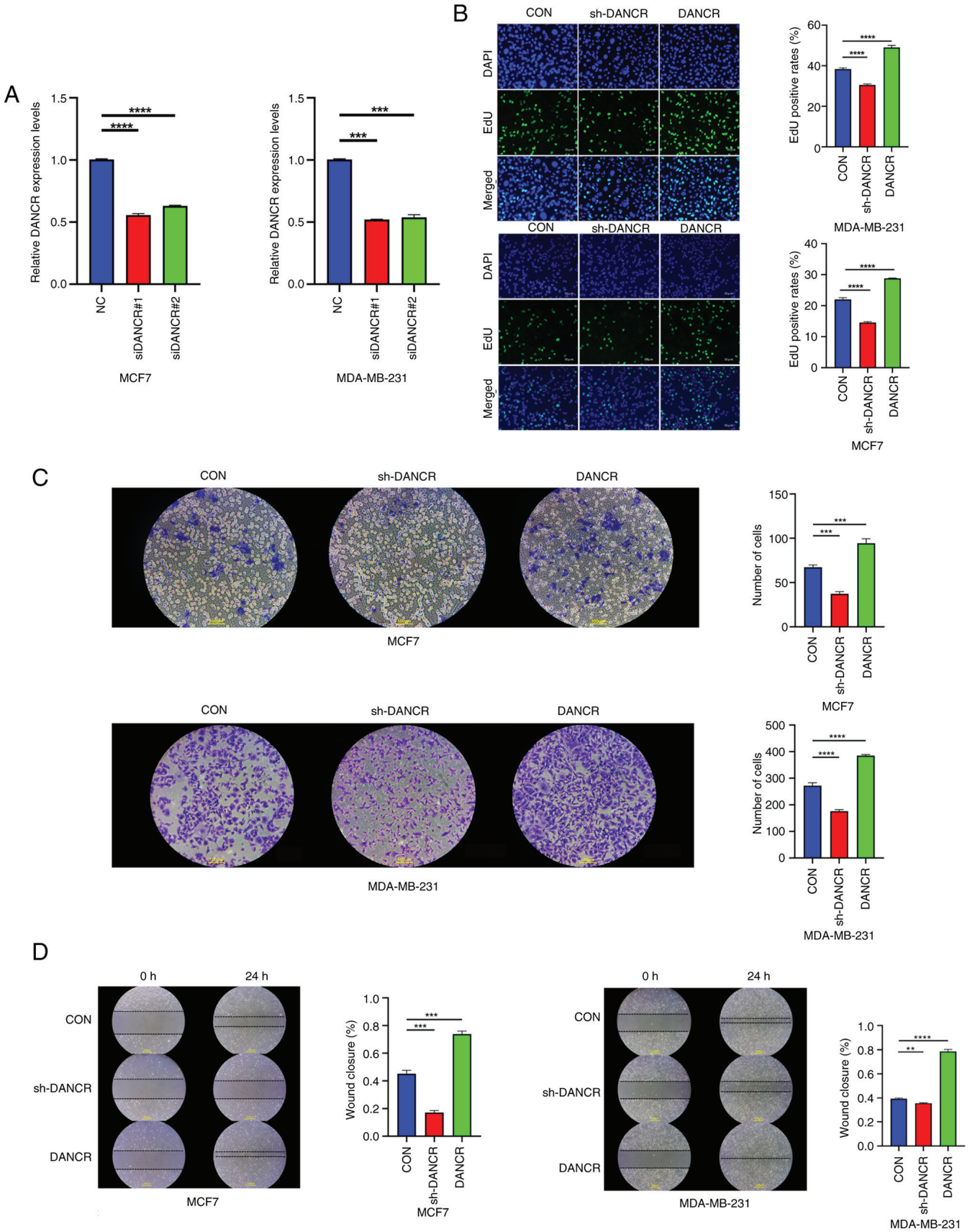

Figure 2. *DANCR* promoted tumor growth. (A) Transfection efficacy of si*DANCR* in MCF7 and MDA-MB-231 cells. (B) EdU assay results demonstrated that silencing *DANCR* inhibited tumor cell proliferation, while overexpression of *DANCR* promoted tumor cell proliferation. Magnification, x100. (C) Transwell invasion assay results showed that knockdown of *DANCR* inhibited the invasion ability of tumor cells, while overexpression of *DANCR* promoted tumor cell invasion ability. Magnification, x200. (D) Wound healing assay results demonstrated that silencing *DANCR* suppressed tumor cell migration, while overexpression of *DANCR* promoted tumor cell migration. Magnification, x100. Data were presented as the mean ± standard deviation (n=3). **P<0.01; ***P<0.001; *****P<0.0001. DANCR, differentiation antagonizing non-protein coding RNA; si, small interfering RNA; sh, short hairpin RNA; NC, negative control; CON, blank control group; EdU, 5-ethynyl-2'-deoxyuridine.

introduction of sh*DANCR* into MCF7 and MDA-MB-231 cells via stable transfection significantly inhibited both invasive and migratory cells compared with control cells (Fig. 2C and D). By contrast, the overexpression of *DANCR* significantly enhanced the invasion (Fig. 2C) and migration (Fig. 2D) of breast cancer cells *in vitro* compared with controls.

DANCR modulated breast cancer cell progression by regulating miR-34c-5p. The typical regulatory role of lncRNAs is to host miRNAs and serve as a miRNA 'sponge'. In the present study, LncLocator and FISH were used to predict and verify the subcellular localization of *DANCR*. The findings demonstrated that the cytoplasm of both the MCF7 and MDA-MB-231 cell lines contained *DANCR* (Fig. 3A and B). Moreover, bioinformatics analysis demonstrated that *miR-34c-5p* contained a sequence matching *DANCR* at the 3'UTR (Fig. 3C). According to the luciferase assay results, *miR-34c-5p* mimics caused a significant decrease in luciferase activity compared with negative controls, which indicated a strong affinity between *DANCR* 3'UTR and *miR-34c* (Fig. 3C). Compared with MCF10A cells, the expression of *miR-34c-5p* was significantly diminished in breast cancer cell lines (Fig. 3D). Additionally, the upregulation of *DANCR* resulted in the downregulation of *miR-34c-5p* (Fig. S3A). The present study indicated that *miR-34c-5p* was negatively correlated with *DANCR* and targeted the 3'UTR of *DANCR*.

Given that *DANCR* has previously been identified as an oncogenic lncRNA in breast cancer (20), how it interacts with *miR-34c-5p* to control pathological course was studied. Loss-of-function and rescue tests were conducted in MCF7 and MDA-MB-231 cells. According to these experiments, si*DANCR* transfection of MCF7 and MDA-MB-231 cells significantly enhanced the expression of *miR-34c-5p* compared with negative controls (Fig. 3E and F). In addition, EdU analysis demonstrated that, compared with in the sh*DANCR* transfection group, sh*DANCR* co-transfection with the *miR-34c-5p* inhibitor significantly reversed the reduced proliferation of MCF7 and MDA-MB-231 breast cancer cells (Fig. 3G). Furthermore, *DANCR* knockdown significantly reduced cell migration and invasion rates compared with controls and this effect was significantly reversed by the *miR-34c-5p* inhibitor (Fig. 3H and I). Overall, these findings suggested a potential antagonistic relationship between *DANCR* and *miR-34c-5p* in breast cancer, whereby *miR-34c-5p* inhibition may help to lessen the inhibitory effect of *DANCR* knockdown on cell proliferation, migration and invasion.

E2F1 acted as the target of miR-34c-5p. *DANCR* expression was shown to be significantly positively correlated with *E2F1* gene expression by bioinformatics analysis (Fig. 4A) and downstream gene pathways, such as *E2F1*, were found to be significantly related to cell cycle and cell division (Fig. 4B). Additionally, it was expected that the 3'UTR of *E2F1* contained binding sites complementary to *miR-34c-5p* (Fig. 4C). The binding of *miR-34c-5p* to the 3'UTR of *E2F1* was confirmed using a luciferase reporter assay (Fig. 4C). These results showed that transfection with the *miR-34c* inhibitor significantly increased *E2F1* expression in MCF7 and MDA-MB-231 cells compared with negative controls (Fig. 4D). In addition, when knocking down *DANCR*, both *E2F1* mRNA and protein expression levels were significantly decreased compared with controls (Fig. 4E and F). However, this effect was reversed when cells were co-transfected with sh*DANCR* and *miR-34c-5p* inhibitor (Fig. 4E and F).

These findings showed a negative association between the expression of *miR-34c-5p* and the expression of *E2F1* and *DANCR*. There was also a strong positive association between *E2F1* expression and *DANCR* expression. Consequently, this study potentially elucidated a regulatory pathways of *DANCR*/*miR-34c-5p*/*E2F1* in breast cancer.

E2F1 regulated the DANCR promoter region and activated its expression. The present study proposed that TF binding to the promoter region of the lncRNA *DANCR* enhanced its expression. To validate this, the online database JASPAR was used to predict TF binding to the *DANCR* promoter region (Fig. 5A). In addition, GO and KEGG analyses were performed to identify the basic functions and pathways of *DANCR* promoter region-binding TFs via DAVID Functional Annotation Bioinformatics Microarray Analysis. These results suggested that the transcription factor *E2F1*, which may serve an important role in breast cancer, could bind to the functional region of the *DANCR* promoter (Fig. 5B). *E2F1* may bind to the promoter region of *DANCR* in MCF7 and MDA-MB-231 breast cancer cell lines. This theory was supported by ChIP-seq data for *E2F1* from ENCODE (Fig. 5C). Additionally, the ChIP data demonstrated that the *DANCR* promoter had a far higher affinity for *E2F1* than for IgG (Fig. 5D).

The pathway by which *DANCR* is upregulated in human cancer was also investigated and it was predicted that cancer samples would have less DNA methylation enrichment at the *DANCR* promoter locus compared with normal samples. In contrast to non-cancer tissues, these findings demonstrated that the *DANCR* promoter region was significantly hypomethylated in pan-cancer, BRCA, BLCA, PRAD and HNSC samples (Figs. 5E and S2; Table SIII). Moreover, in pan-cancer samples and most types of malignancies tested, the degree of *DANCR* promoter region methylation was significantly inversely correlated with *DANCR* expression (Figs. 5F and S2; Tables SIII and SIV).

Additionally, the role of H3K27ac and H3K4me3 modifications in upregulating *DANCR* expression in human cancer was investigated. These results demonstrated that both modifications were significantly enriched at the *DANCR* locus in breast cancer cell lines (Fig. 5G), which indicated their potential contribution to the upregulation of *DANCR* in breast cancer. Taken together, these findings suggested that TF binding, hypomethylation and H3K27ac and H3K4me3 modifications may collectively contribute to the upregulation of *DANCR* in breast cancer.

Discussion

In human esophageal squamous cell carcinoma and osteosarcoma, the lncRNA *DANCR* serves a crucial role, according to previously published studies (21,22). *DANCR* upregulation has been identified as a prognostic biomarker in both pancreatic and colorectal cancer (23,24). In our previous research, we reported that *DANCR* serves a tumor-promoting role both *in vivo* and *in vitro* in breast cancer (20). Mechanistically, *DANCR* targets

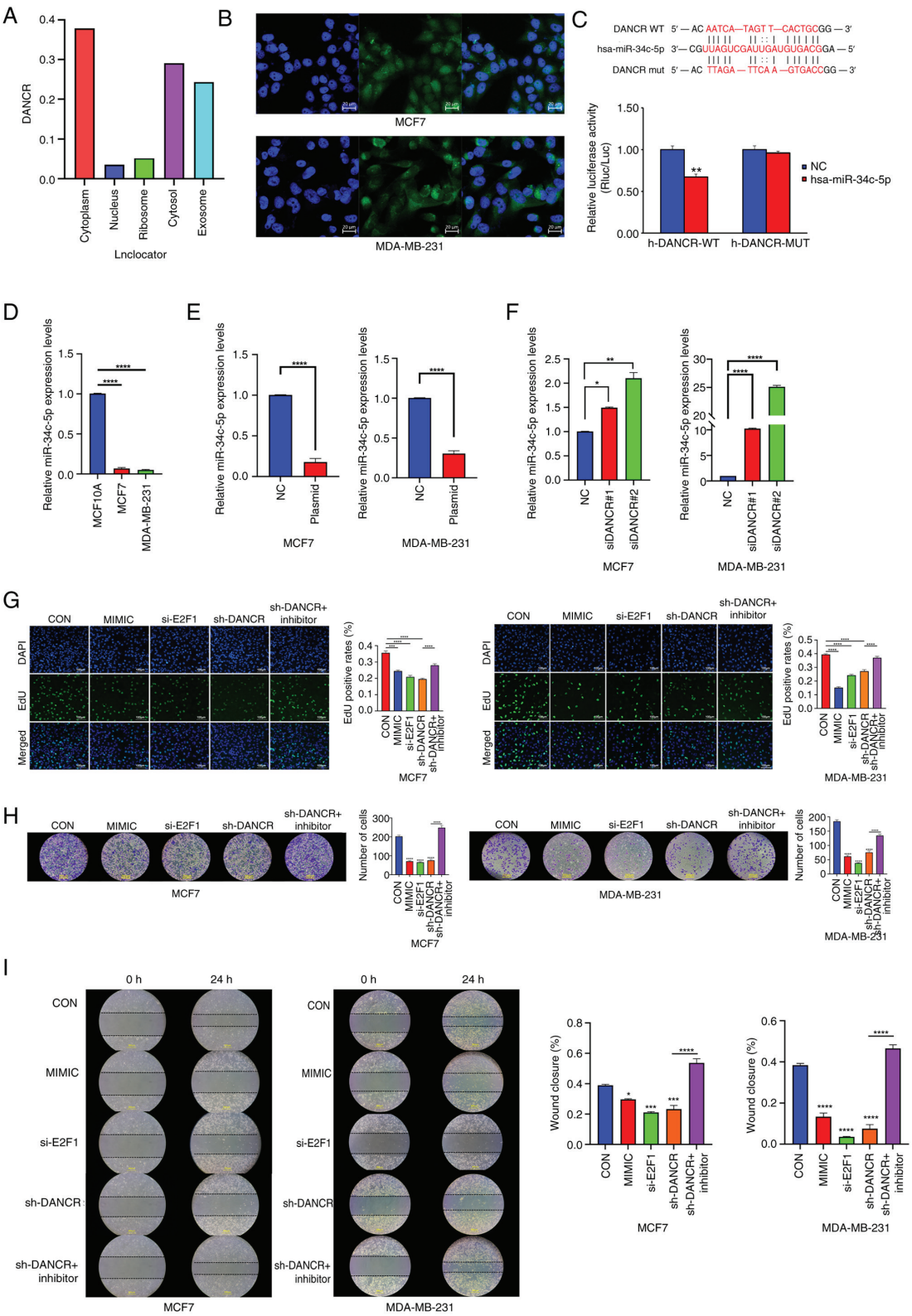

Figure 3. *DANCR* modulated breast cancer cells progression via regulating *miR-34c-5p*. (A) Lnclocator predicted that *DANCR* was mainly located in the MCF7 cytoplasm. (B) Distribution of *DANCR* (green) in MCF7 and MDA-MB-231 cells as detected by fluorescence *in situ* hybridization assay (nuclei stained blue with DAPI). Magnification, x400. (C) A luciferase reporter assay was used to assess the interactions between *miR-34c-5p* and its binding sites or mutated binding sites in the 3' untranslated regions of *DANCR* in 293T cells. (D) Expression levels of *miR-34c-5p* were higher in breast cancer cell lines compared with the MCF10A cell line. (E) Overexpression of *DANCR* upregulated the expression level of *miR-34c-5p*. (F) Knockdown of *DANCR* downregulated the expression level of *miR-34c-5p*. (G) The proliferation capacity of *miR-34c-5p* mimic, *E2F1* siRNA, *DANCR* shRNA and *DANCR* shRNA + miR-34c inhibitor transfected MCF7 and MDA-MB-231 cells were assessed by EdU assay. Magnification, x100. (H) The invasion capacity of *miR-34c-5p* mimic, *E2F1* siRNA, *DANCR* shRNA and *DANCR* shRNA plus miR-34c inhibitor transfected MCF7 and MDA-MB-231 cells were assessed by Transwell assay. Magnification, x200. (I) The migratory capacity of *miR-34c-5p* mimic, *E2F1* siRNA, *DANCR* shRNA and *DANCR* shRNA + miR-34c inhibitor transfected MCF7 and MDA-MB-231 cells were assessed by wound healing assay. Magnification, x100. Data were presented as the mean ± standard deviation (n=3). *P<0.05; **P<0.01; ***P<0.001; *****P<0.0001. DANCR, differentiation antagonizing non-protein coding RNA; E2F1, E2F transcription factor 1; WT, wild type; mut, mutant; miR, microRNA; si, small interfering RNA; sh, short hairpin RNA; NC, negative control; CON, blank control group.

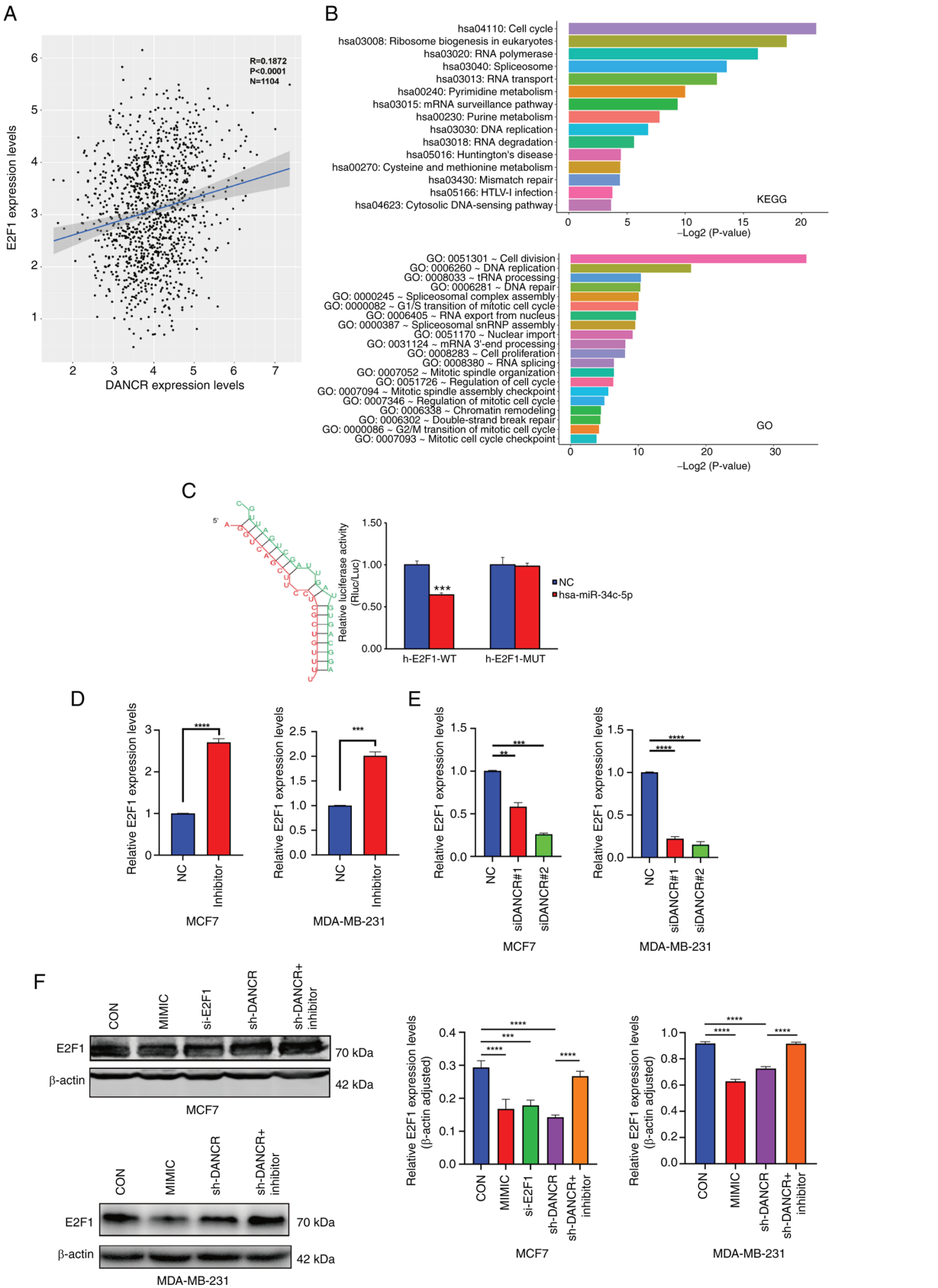

Figure 4. *E2F1* acted as the target of *miR-34c-5p*. (A) The Cancer Genome Atlas data showed that *E2F1* positively correlated with *DANCR* in breast cancer. (B) GO and KEGG enrichment analysis of key genes of *DANCR* downstream pathway. (C) A luciferase reporter assay was used to assess the interactions between *miR-34c-5p* and its binding sites or mutated binding sites in the 3' untranslated regions of *E2F1* in 293T cells. (D) Downregulated *miR-34c-5p* promoted *E2F1* expression. (E) Knockdown of *DANCR* upregulated the expression levels of *E2F1*. (F) *E2F1* expression changes cells transfected with in miR-34c mimic, *DANCR* shRNA and *DANCR* shRNA + miR-34c inhibitor as detected by Western blotting. Data were presented as the mean ± standard deviation (n=3). **P<0.01; ***P<0.001; *****P<0.0001. DANCR, differentiation antagonizing non-protein coding RNA; E2F1, E2F transcription factor 1; WT, wild type; MUT, mutant; miR, microRNA; si, small interfering RNA; sh, short hairpin RNA; KEGG, Kyoto Encyclopedia of Genes and Genomes; GO, Gene Ontology; NC, negative control; CON, blank control group.

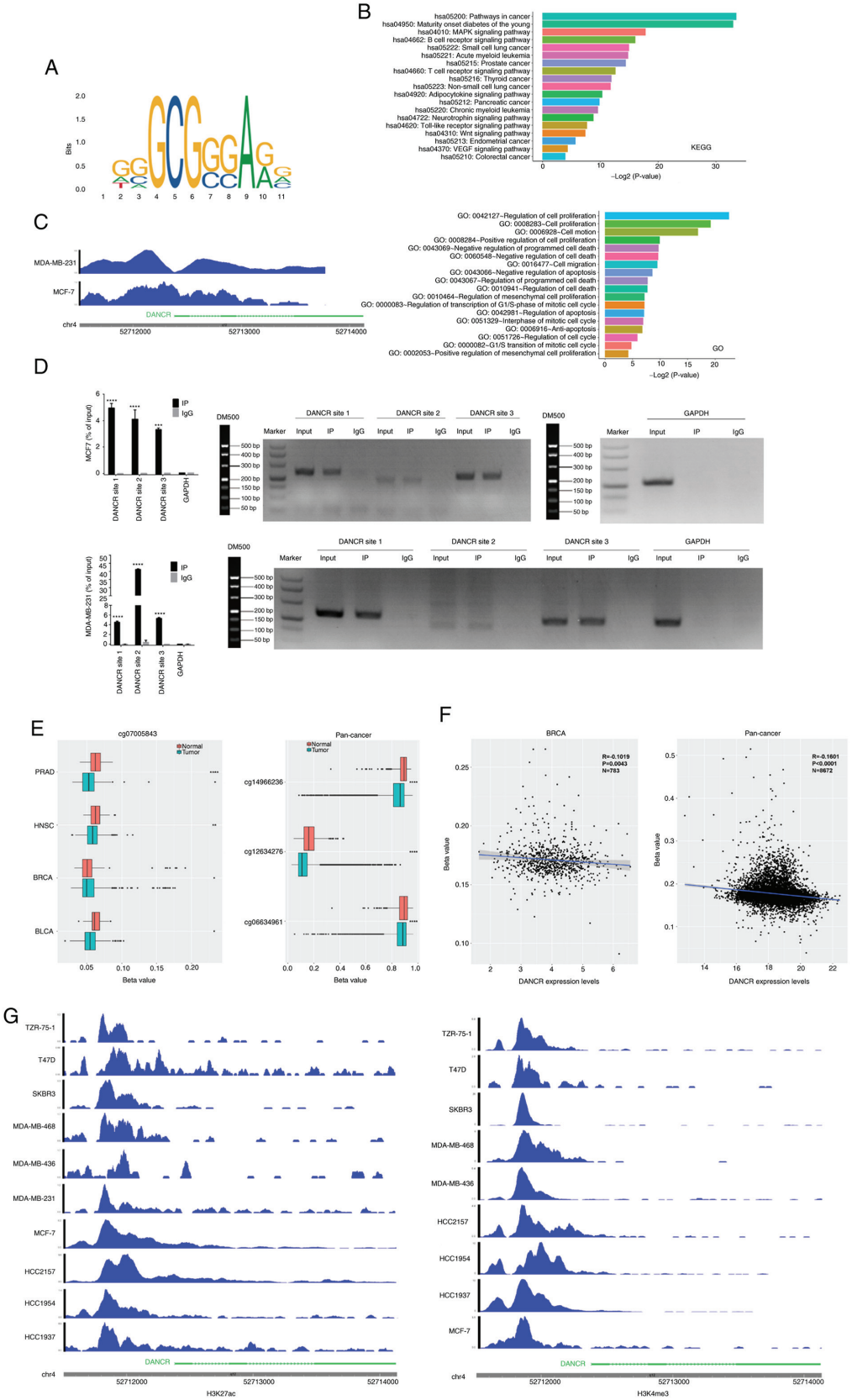

Figure 5. *E2F1* regulated the *DANCR* promoter region and activates its expression. (A) JASPAR predicted that *E2F1* could bind with the promoter of *DANCR*. (B) GO/KEGG enrichment analysis of transcription factors predicted to bind to *DANCR*. (C) ENCODE validated the binding region of *E2F1* to the *DANCR* promoter. (D) Chromatin immunoprecipitation assay showed the binding of *E2F1* and *DANCR* promoter region in MCF7 and MDA-MB-231 cells. Data were presented as the mean ± standard deviation (n=3). (E) Hypomethylation occurred at the *DANCR* promoter locus in breast and pan-cancer tissues. (F) The methylation level at the *DANCR* promoter site was inversely proportional to *DANCR* expression in breast and pan-cancer samples. (G) H3K27ac and H3K4me3 were significantly enriched at the *DANCR* locus in breast cancer cell lines. *P<0.05; **P<0.01; ***P<0.001; ****P<0.0001. DANCR, differentiation antagonizing non-protein coding RNA; E2F1, E2F transcription factor 1; KEGG, Kyoto Encyclopedia of Genes and Genomes; GO, Gene Ontology; PRAD, prostate adenocarcinoma; HNSC, head and neck squamous cell carcinoma; BRCA, breast invasive carcinoma; BLCA, bladder urothelial carcinoma; bp, base pairs; IP, immunoprecipitation group; DM500, DNA marker.

miR-216a-5p, thereby regulating the expression of proteins such as Nanog, SOX2 and OCT4 to promote breast cancer progression. In the present study, the results demonstrated that partial inhibition of *DANCR* significantly reduced the proliferation, migration and invasion of MDA-MB-231 and MCF7 cells, which may have an impact on the tumor cell cycle.

Previous research has indicated that lncRNAs are involved in the epigenetic modification of multiple diseases, including via both transcriptional and post-transcriptional regulation (25,26). Notably, it has been reported that lncRNAs serve a crucial role in the etiology, proliferation, metastasis and recurrence of tumors (27-30). Currently, the most well-known mechanism by which lncRNAs participate in disease etiology is by serving as ceRNAs for miRNAs (31,32). In the present study, through computational approaches, it was determined that *miR-34c-5p* bound to the 3'UTR of *DANCR*. Furthermore, functional experiments showed the ability of *miR-34c-5p* to inhibit the oncogenic effects of *DANCR* on breast cancer cells, which suggests that the regulatory effect of *DANCR* on these cells may be mediated by its sequestration of *miR-34c-5p*. The regulation of gene expression by miRNAs occurs through binding to particular locations in the 3'UTR of target mRNAs and lncRNA-miRNA crosstalk is essential for the indirect control of gene expression (33-36). When lncRNAs are in the cytoplasm, they participate in modulating mRNA stability, regulating mRNA translation, serving as ceRNAs and functioning as precursors of miRNAs (31). In the present study, the subcellular grading confirmed that DANCR is mainly located in the cytoplasm of breast cancer cell lines. Furthermore, the inhibitory effect of shDANCR on *E2F1* could be reversed by miR-34c-5p inhibitor, which suggests that DANCR could potentially enhance the expression of *E2F1* by absorbing miR-34c-5p as ceRNA in cancer. Additionally, the present study demonstrated the involvement of the *DANCR/miR-34c-5p/E2F1* feedback loop in the occurrence and development of breast cancer (Fig. 6). By modulating the expression of the oncogene *E2F1*, *DANCR* may serve as a potential therapeutic target for breast cancer. The results of the present study suggested that manipulating the expression of *DANCR*, as a ceRNA, may competitively regulate the expression of *E2F1*, thereby regulating the biological function of breast cancer cells. However, in the future, additional *in vivo* experiments and clinical trials are necessary to clarify the potential of *DANCR* as a therapeutic target for breast cancer.

The results of the present study showed that knocking down *E2F1* reduced cell migration and invasion. Therefore, *E2F1*, as a protein regulated by *DANCR*, may be involved in the G_1/S transition of the mitochondrial cell cycle, regulation of the cell cycle, regulation of the mitochondrial cell cycle and G_2/M transition of the mitochondrial cell cycle. *E2F1*, as a TF that binds to the *DANCR* promoter region, may be involved in the regulation of transcription of G_1/S phase of the mitotic cell cycle, interphase of the mitotic cell cycle, cell cycle regulation, G_1/S transition of the mitotic cell cycle and the G_1 phase of the mitotic cell cycle.

Based on the analysis of the binding region between the TF *E2F1* and *DANCR*, further analysis was performed on biological behaviors that *E2F1* may be involved in by activating *DANCR* transcription. These results demonstrated that the regulation of *DANCR* by the TF *E2F1* may be involved in various types of cancer, such as small cell lung cancer, prostate cancer and thyroid cancer, as well as signaling pathways,

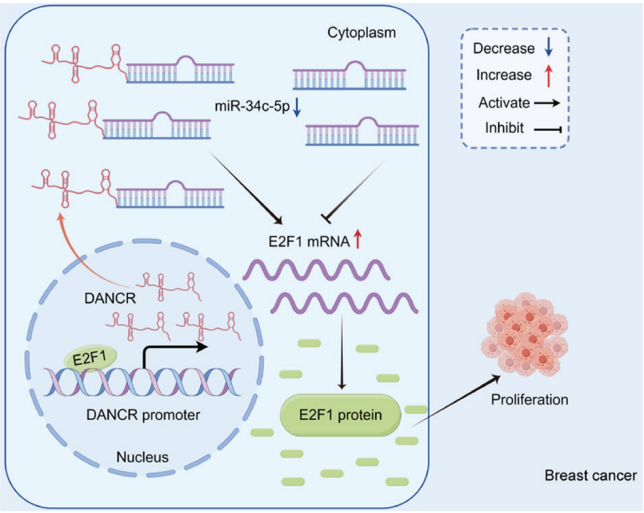

Figure 6. Role of *DANCR* in breast cancer progression in the present study. The transcription factor *E2F1* could bind to the promoter region of *DANCR*, activating its transcription. *DANCR*, in turn, promoted the progression of breast cancer by competitively binding with *miR-34c-5p*, which led to the upregulation of *E2F1* expression. DANCR, differentiation antagonizing non-protein coding RNA; E2F1, E2F transcription factor 1; miR, microRNA.

such as the *MAPK* signaling pathway, the Toll-like receptor pathway and the *Wnt* signaling pathway. Furthermore, *E2F1* may be involved in regulating cell proliferation, cell death and the cell cycle. Therefore, it could potentially be hypothesized that the TF *E2F1* binds to the *DANCR* promoter functional region and serves an important role in cancer.

Our previous study reported that *miR-34c-5p* can mediate liver and lung metastasis of breast cancer by regulating G protein-coupled receptor kinase interacting protein 1 (GIT1) (37). In addition, GIT1 can mediate the development of estrogen receptor-negative breast cancer by regulating the *Notch* pathway (38). Another study reported that UBTF promotes melanoma cell proliferation and cell cycle progression by promoting GIT1 transcription, thereby activating MEK1/2-ERK1/2 signaling pathways (39). Therefore, *E2F1* and *miR-34c-5p* may regulate the progression of breast cancer by affecting the cell cycle.

Further validation of the present findings are required to address a number of limitations of the present study. Firstly, it is imperative to note that the assessment of *DANCR* expression levels in a limited sample size of breast cancer specimens requires further investigation with a more extensive sample size to establish a definitive correlation between the expression of *DANCR/miR-34c/E2F1* and clinical parameters. Furthermore, it is necessary to confirm the protein concentration of *E2F1* and the expression level of *DANCR* across a wider range of cell models and *in vivo* studies. Finally, the genes of interest identified in the present study via bioinformatics analysis, which may have the potential to become significant contributors to the development of breast cancer, warrant further investigation to validate the results.

Nevertheless, the present study demonstrated the potential role of *DANCR* in breast cancer progression. The formation of the *DANCR/miR-34c/E2F1* feedback loop, facilitated by the binding of *E2F1* to the *DANCR* promoter region, may provide a promising avenue for the precise treatment of breast cancer in the future.

Acknowledgements

Not applicable.

Funding

This work was supported by the First Affiliated Hospital of Harbin Medical University Fund for Distinguished Young Medical Scholars (grant no. 2021J17), the Beijing Medical Award Foundation (grant no. YXJL-2021-0302-0287), and the Postgraduate Research and Practice Innovation Program of Harbin Medical University (grant no. YJSCX2023-63HYD).

Availability of data and materials

The datasets used and/or analyzed during the current study are available from the corresponding author on reasonable request.

Authors' contributions

SY and WT confirm the authenticity of all the raw data. SY and WT designed and directed experimental studies. SY, LT, JD, LJ, PX, WZ and WT performed sequencing data analysis. SY, LT, JD, LJ, PX and WZ performed experimental studies. SY, LJ and WT acquired patient samples. WT provided financial support. SY and WT provided project guidance. SY, LT, JD, LJ, PX, WZ and WT wrote the manuscript, which all authors reviewed. All authors read and approved the final version of the manuscript.

Ethics approval and consent to participate

The First Hospital of Harbin Medical University granted ethical approval for the present study and all patients provided their written informed consent (approval no.: 202438; Harbin, China).

Patient consent for publication

Not applicable.

Competing interests

The authors declare that they have no competing interests.

References

1. Sung H, Ferlay J, Siegel RL, Laversanne M, Soerjomataram I, Jemal A and Bray F: Global Cancer Statistics 2020: GLOBOCAN estimates of incidence and mortality worldwide for 36 cancers in 185 countries. CA Cancer J Clin 71: 209-249, 2021.
2. Ramamoorthi G, Kodumudi K, Gallen C, Zachariah NN, Basu A, Albert G, Beyer A, Snyder C, Wiener D, Costa RLB and Czerniecki BJ: Disseminated cancer cells in breast cancer: Mechanism of dissemination and dormancy and emerging insights on therapeutic opportunities. Semin Cancer Biol 78: 78-89, 2022.
3. Zhu L, Jiang S, Yu S, Liu X, Pu S, Xie P, Chen H, Liao X, Wang K and Wang B: Increased SIX-1 expression promotes breast cancer metastasis by regulating lncATB-miR-200s-ZEB1 axis. J Cell Mol Med 24: 5290-5303, 2020.
4. Zhu L, Tian Q, Gao H, Wu K, Wang B, Ge G, Jiang S, Wang K, Zhou C, He J, *et al*: PROX1 promotes breast cancer invasion and metastasis through WNT/β-catenin pathway via interacting with hnRNPK. Int J Biol Sci 18: 2032-2046, 2022.
5. Jiang W, Xia J, Xie S, Zou R, Pan S, Wang ZW, Assaraf YG and Zhu X: Long non-coding RNAs as a determinant of cancer drug resistance: Towards the overcoming of chemoresistance via modulation of lncRNAs. Drug Resist Updat 50: 100683, 2020.
6. Chu Z, Huo N, Zhu X, Liu H, Cong R, Ma L, Kang X, Xue C, Li J, Li Q, *et al*: FOXO3A-induced LINC00926 suppresses breast tumor growth and metastasis through inhibition of PGK1-mediated Warburg effect. Mol Ther 29: 2737-2753, 2021.
7. Huang Y, Mo W, Ding X and Ding Y: Long non-coding RNAs in breast cancer stem cells. Med Oncol 40: 177, 2023.
8. Karthikeyan SK, Xu N, Ferguson Rd JE, Rais-Bahrami S, Qin ZS, Manne U, Netto GJ, S Chandrashekar D and Varambally S: Identification of androgen response-related lncRNAs in prostate cancer. Prostate 83: 590-601, 2023.
9. Chen X, Luo R, Zhang Y, Ye S, Zeng X, Liu J, Huang D, Liu Y, Liu Q, Luo ML, *et al*: Long noncoding RNA DIO3OS induces glycolytic-dominant metabolic reprogramming to promote aromatase inhibitor resistance in breast cancer. Nat Commun 13: 7160, 2022.
10. Zhou L, Jiang J, Huang Z, Jin P, Peng L, Luo M, Zhang Z, Chen Y, Xie N, Gao W, *et al*: Hypoxia-induced lncRNA STEAP3-AS1 activates Wnt/β-catenin signaling to promote colorectal cancer progression by preventing m^6A-mediated degradation of STEAP3 mRNA. Mol Cancer 21: 168, 2022.
11. Tong X, Gu PC, Xu SZ and Lin XJ: Long non-coding RNA-DANCR in human circulating monocytes: A potential biomarker associated with postmenopausal osteoporosis. Biosci Biotechnol Biochem 79: 732-737, 2015.
12. Gan X, Ding D, Wang M, Yang Y, Sun D, Li W, Ding W, Yang F, Zhou W and Yuan S: DANCR deletion retards the initiation and progression of hepatocellular carcinoma based on gene knockout and patient-derived xenograft in situ hepatoma mice model. Cancer Lett 550: 215930, 2022.
13. Lamere AT and Li J: Inference of gene co-expression networks from single-cell RNA-sequencing data. Methods Mol Biol 1935: 141-153, 2019.
14. Luo ZH, Walid AA, Xie Y, Long H, Xiao W, Xu L, Fu Y, Feng L and Xiao B: Construction and analysis of a dysregulated lncRNA-associated ceRNA network in a rat model of temporal lobe epilepsy. Seizure 69: 105-114, 2019.
15. Ruan Y, Li Y, Liu Y, Zhou J, Wang X and Zhang W: Investigation of optimal pathways for preeclampsia using network-based guilt by association algorithm. Exp Ther Med 17: 4139-4143, 2019.
16. Thiel D, Conrad ND, Ntini E, Peschutter RX, Siebert H and Marsico A: Identifying lncRNA-mediated regulatory modules via ChIA-PET network analysis. BMC Bioinformatics 20: 292, 2019.
17. Livak KJ and Schmittgen TD: Analysis of relative gene expression data using real-time quantitative PCR and the 2(-Delta Delta C(T)) method. Methods 25: 402-408, 2001.
18. Zhong G, Su S, Li J, Zhao H, Hu D, Chen J, Li S, Lin Y, Wen L, Lin X, *et al*: Activation of Piezo1 promotes osteogenic differentiation of aortic valve interstitial cell through YAP-dependent glutaminolysis. Sci Adv 9: eadg0478, 2023.
19. Xiao YF, Li BS, Liu JJ, Wang SM, Liu J, Yang H, Hu YY, Gong CL, Li JL and Yang SM: Role of lncSLCO1C1 in gastric cancer progression and resistance to oxaliplatin therapy. Clin Transl Med 12: e691, 2022.
20. Tao W, Wang C, Zhu B, Zhang G and Pang D: LncRNA DANCR contributes to tumor progression via targetting miR-216a-5p in breast cancer: lncRNA DANCR contributes to tumor progression. Biosci Rep 39: BSR20181618, 2019.
21. Bi Y, Guo S, Xu X, Kong P, Cui H, Yan T, Ma Y, Cheng Y, Chen Y, Liu X, *et al*: Decreased ZNF750 promotes angiogenesis in a paracrine manner via activating DANCR/miR-4707-3p/FOXC2 axis in esophageal squamous cell carcinoma. Cell Death Dis 11: 296, 2020.
22. Pan Z, Wu C, Li Y, Li H, An Y, Wang G, Dai J and Wang Q: LncRNA DANCR silence inhibits SOX5-medicated progression and autophagy in osteosarcoma via regulating miR-216a-5p. Biomed Pharmacother 122: 109707, 2020.
23. Hu X, Peng WX, Zhou H, Jiang J, Zhou X, Huang D, Mo YY and Yang L: IGF2BP2 regulates DANCR by serving as an N6-methyladenosine reader. Cell Death Differ 27: 1782-1794, 2020.
24. Xiong M, Wu M, Peng D, Huang W, Chen Z, Ke H, Chen Z, Song W, Zhao Y, Xiang AP, *et al*: LncRNA DANCR represses Doxorubicin-induced apoptosis through stabilizing MALAT1 expression in colorectal cancer cells. Cell Death Dis 12: 24, 2021.

25. Zhang X, Xie K, Zhou H, Wu Y, Li C, Liu Y, Liu Z, Xu Q, Liu S, Xiao D and Tao Y: Role of non-coding RNAs and RNA modifiers in cancer therapy resistance. Mol Cancer 19: 47, 2020.
26. Yang ZJ, Liu R, Han XJ, Qiu CL, Dong GL, Liu ZQ, Liu LH, Luo Y and Jiang LP: Knockdown of the long non-coding RNA MALAT1 ameliorates TNF-α-mediated endothelial cell pyroptosis via the miR-30c-5p/Cx43 axis. Mol Med Rep 27: 90, 2023.
27. Shi SJ, Wang LJ, Yu B, Li YH, Jin Y and Bai XZ: LncRNA-ATB promotes trastuzumab resistance and invasion-metastasis cascade in breast cancer. Oncotarget 6: 11652-11663, 2015.
28. Xue X, Yang YA, Zhang A, Fong KW, Kim J, Song B, Li S, Zhao JC and Yu J: LncRNA HOTAIR enhances ER signaling and confers tamoxifen resistance in breast cancer. Oncogene 35: 2746-2755, 2016.
29. Ghafouri-Fard S, Khoshbakht T, Hussen BM, Baniahmad A, Taheri M and Samadian M: A review on the role of DANCR in the carcinogenesis. Cancer Cell Int 22: 194, 2022.
30. Xu Y, Bao Y, Qiu G, Ye H, He M and Wei X: METTL3 promotes proliferation and migration of colorectal cancer cells by increasing SNHG1 stability. Mol Med Rep 28: 217, 2023.
31. Xue ST, Zheng B, Cao SQ, Ding JC, Hu GS, Liu W and Chen C: Long non-coding RNA LINC00680 functions as a ceRNA to promote esophageal squamous cell carcinoma progression through the miR-423-5p/PAK6 axis. Mol Cancer 21: 69, 2022.
32. Ghaemi Z, Mowla SJ and Soltani BM: Novel splice variants of LINC00963 suppress colorectal cancer cell proliferation via miR-10a/miR-143/miR-217/miR-512-mediated regulation of PI3K/AKT and Wnt/β-catenin signaling pathways. Biochim Biophys Acta Gene Regul Mech 1866: 194921, 2023.
33. Yang S, Wang X, Zhou X, Hou L, Wu J, Zhang W, Li H, Gao C and Sun C: ncRNA-mediated ceRNA regulatory network: Transcriptomic insights into breast cancer progression and treatment strategies. Biomed Pharmacother 162: 114698, 2023.
34. Zhou Y, Meng X, Chen S, Li W, Li D, Singer R and Gu W: IMP1 regulates UCA1-mediated cell invasion through facilitating UCA1 decay and decreasing the sponge effect of UCA1 for miR-122-5p. Breast Cancer Res 20: 32, 2018.
35. Jiang N, Wang X, Xie X, Liao Y, Liu N, Liu J, Miao N, Shen J and Peng T: lncRNA DANCR promotes tumor progression and cancer stemness features in osteosarcoma by upregulating AXL via miR-33a-5p inhibition. Cancer Lett 405: 46-55, 2017.
36. Lu G, Li Y, Ma Y, Lu J, Chen Y, Jiang Q, Qin Q, Zhao L, Huang Q, Luo Z, *et al*: Long noncoding RNA LINC00511 contributes to breast cancer tumourigenesis and stemness by inducing the miR-185-3p/E2F1/Nanog axis. J Exp Clin Cancer Res 37: 289, 2018.
37. Tao WY, Wang CY, Sun YH, Su YH, Pang D and Zhang GQ: MicroRNA-34c suppresses breast cancer migration and invasion by targeting GIT1. J Cancer 7: 1653-1662, 2016.
38. Zhang S, Miyakawa A, Wickström M, Dyberg C, Louhivuori L, Varas-Godoy M, Kemppainen K, Kanatani S, Kaczynska D, Ellström ID, *et al*: GIT1 protects against breast cancer growth through negative regulation of Notch. Nat Commun 13: 1537, 2022.
39. Zhang J, Zhang J, Liu W, Ge R, Gao T, Tian Q, Mu X, Zhao L and Li X: UBTF facilitates melanoma progression via modulating MEK1/2-ERK1/2 signalling pathways by promoting GIT1 transcription. Cancer Cell Int 21: 543, 2021.